Chem. Senses 24: 679–690, 1999

A Functional Map in Rat Olfactory Epithelium

John W. Scott and Tracy Brierley

Department of Cell Biology, Emory University School of Medicine, Atlanta, GA 30322-3030, USA

Correspondence to be sent to: John W. Scott, Department of Cell Biology, Emory University School of Medicine, Atlanta, GA 30322-3030, USA. e-mail johns@cellbio.emory.edu

Abstract

Multiple (four or eight) electrode arrays were placed for simultaneous electro-olfactogram (EOG) recordings of responses to a series of odors applied directly to the olfactory epithelium. Three different surfaces of the epithelium were exposed in rats immediately after death by anesthetic overdose. We tested three terpene compounds (carvone, limonene and 1,8-cineole) across the epithelium along the medial surface of the endoturbinate bones. Carvone, a ketone, evoked larger responses dorsally on the epithelium. The largest responses to 1,8-cineole (an ether) were seen in an intermediate-ventral region. The responses to limonene (a hydrocarbon) did not vary greatly across the regions, although they were often larger ventrally. The response distributions deviated from this simple pattern on the caudal part of endoturbinate IV, where the carvone responses were small and the limonene responses were larger. These differences were evident across a substantial concentration range. Similar distributions were seen for these three odors in tests along the dorsal-to-ventral direction across the nasal septum and in the medial-to-lateral direction across the dorsal aspect of one of the endoturbinate bones reaching out into the lateral recess. We argue that the spatial distributions of responses are correlated with the olfactory receptor gene expression zones.

Introduction

The question of regional specificity of mammalian olfactory receptors is still an important one. Although axons from cells expressing the same receptor gene converge onto a single set of olfactory bulb glomeruli in rodents (Ressler *et al.*, 1994; Vassar *et al.*, 1994; Mombaerts *et al.*, 1996), this convergence is limited by the organization of the olfactory epithelium. Receptor cells expressing any particular olfactory receptor gene are usually found within one of four longitudinal zones within the olfactory epithelium of rats and mice (Nef *et al.*, 1992; Ressler *et al.*, 1993; Vassar *et al.*, 1993; Strotmann *et al.*, 1994; Wang *et al.*, 1998). This convergence is consistent with physiological evidence suggesting that each glomerulus may receive a different sampling of information about the olfactory environment (Leveteau and MacLeod, 1966; Lancet *et al.*, 1981; Imamura *et al.*, 1992; Guthrie *et al.*, 1993; Mori and Yoshihara, 1995; Bozza and Kauer, 1998). Our laboratory has used multiple electrode electro-olfactograms (EOGs) to describe regional olfactory sensitivity in the rodent olfactory epithelium (Ezeh *et al.*, 1995; Scott *et al.,* 1996). We drew parallels between the distribution of odor responses and the expression zones for olfactory receptor genes (Scott *et al.*, 1997).

The regional localization of odor sensitivity suggests that there is a general pattern of olfactory information entering the olfactory bulb. This pattern is consistent with the broad regional differences in the sensitivity of neurons in the olfactory bulb (Mori and Yoshihara, 1995) and with the projection patterns from the receptor cells to the bulb (Pedersen *et al.*, 1986; Astic *et al.*, 1987; Schoenfeld *et al.*, 1994). However, other recent reports of recordings from the rat olfactory epithelium (Mackay-Sim and Kesteven, 1994; Youngentob *et al.*, 1995) do not support response gradients that correlate with the gene expression zones. Therefore, we have tested a broader range of stimulus concentrations and of epithelial surfaces to carefully re-evaluate our earlier findings.

The recordings in the present study were taken from several surfaces of the olfactory epithelium. The primary set of sites was along the medial surface of three of the endoturbinate bones. Other recordings were from the nasal septum or the dorsal surface of one endoturbinate bone. These sites exposed regions corresponding to the four gene expression zones, but in different locations. For more precise localization, we increased the number of recording electrodes to eight for many of these recordings. With this eight-electrode array, we tested whether the response profile shifted systematically with concentration and tested for discontinuities between the expression zones. By charting the positions of the recordings in each animal, we made composite curves based on a large series of points in the epithelium. This allowed the combination of points from multiple animals to test whether the response profiles follow the gene expression zones. We tested a series of

© Oxford University Press 1999

concentrations at each recording site and explored several classes of odorant compounds on some of these sites.

Materials and methods

Surgical preparation

Male Sprague–Dawley rats (375–525 g) were killed with an overdose of Nembutal (20 mg/kg). We exposed the olfactory epithelium overlying the medial surface of the endoturbinate bones on the left side, as in our previous paper (Scott *et al.*, 1997). The endoturbinate bones are the protrusions of the ethmoid bones that extend closest to the midline of the nasal cavity. The entire region from endoturbinate II to endoturbinate IV was exposed from the dorsal margin at the cribriform plate to the ventral margin at the respiratory epithelium. Room temperature was kept at ~17°C to prolong the usefulness of the preparation. A constant flow of humidified air (1000 ml/min) was immediately established with an 8 mm tube positioned 2 cm from the epithelial surface. This tube was centered on the recording area at an angle of ~30°. In our previous paper (Scott *et al.*, 1997), we could detect no influence of the tube angle on the differential distribution of odor responses.

In four sessions, we also explored the epithelium on the nasal septum. In seven others, we explored the dorsal aspect of endoturbinate II after removing the roof of the nasal cavity and the overlying ectoturbinate bones. This allowed us to test whether the apparent correlation with the gene expression zones extended into the lateral recesses of the nasal cavity.

Recording procedure

An indifferent electrode (a silver chloride electrode connected by an agar bridge to a saline-soaked cotton pad) was placed on the frontal bone overlying the left olfactory bulb. Recordings were made with eight glass micropipettes filled with agar made up in Ringer's solution. These micropipettes were broken to a resistance of <5 MΩ. The leads from these electrodes were connected to two four-channel AC coupled amplifiers (low-frequency time constant 0.1 Hz). The electrode placements were usually along the rostral borders of the turbinate bones, but other placements, particularly the caudal parts of endoturbinate IV, were also explored. Figure 1A shows the exposure of the medial wall of the endoturbinate bones and illustrates the terms that we will use to describe electrode orientation. Placement of the electrodes was monitored by listening to an audio monitor output from the amplifiers to fix the electrodes at the point of first contact with the tissue. This should place the electrode at the mucosal surface and give the maximal response amplitude. It is likely, however, that some electrodes advanced into the tissue slightly as others were being set. For this reason, the eight-electrode configuration was less stable than the four-electrode configuration that we used previously (Scott *et al.*, 1997). Figure 1B illustrates examples of EOGs from eight electrode recordings and illustrates variation in response size that may have arisen in part from electrode movement during placement. Figure 1C shows peak voltage responses to isoamyl acetate across all the initial placements along the rostral border of endoturbinate II′. In some of these cases, repositioning of the electrode led to larger responses. Nevertheless, the great variation shows the necessity for the response standardization described below. On average the isoamyl acetate response was slightly larger ventrally, but the difference was not statistically significant. The electrode array was usually left in place during a complete recording session, but occasionally two sets of placements were used during a single experiment. The lateral set of recordings was done on a different set-up with only four electrodes.

Odor stimulation

Odor concentration was generated by an air dilution olfactometer and concentration was expressed as a proportion of air saturated with odorant. Odor dilutions were generated by using a syringe pump to force air through the head space in glass bottles in which 2–5 ml of the pure odorant were used to cover the bottom. The four tubes were connected by Teflon tubes to ports in the glass tube next to the epithelium. The rate of this flow through the odorant bottle, divided by the 1000 ml/min flow in the stimulus tube, determined the dilution.

The output of this system was evaluated by drawing the stimulus into a gas chromatograph with a flame ionization detector and a DC-200 column (Gow-Mac, Bethlehem, PA). Odors were drawn into a gas sampling valve from the port of the olfactometer. The gas chromatograph was calibrated by diluting known amounts of the odorant chemicals in hexane, which came off the column very rapidly. The output of the flame ionization detector was fed into the A/D converter and area under the curve was measured with a statistical package. These tests showed that the estimated odor concentration was close to the value observed with the gas chromatograph (Table 1). Calculated concentrations in that table were estimated from the vapor pressure at 17°C by dividing that vapor pressure by the atmospheric pressure. That ratio tells the fraction of the mixture contributed by the odor vapor. That ratio was divided by the number of liters occupied by a mole of gas at standard temperature and pressure, and adjusted for the room temperature, to give the number of moles per liter. We also found that the system was reliable down to a dilution of 1×10^{-4}. We can observe reliable isoamyl acetate responses in the EOG at that dilution. The data figures will express odor concentration in terms of dilution rather than the estimated moles per liter.

A BASIC language program controlled the pump rate and set valves to inject each odor. This program used a standard file to determine the odor sequence and their concentrations. Each set of three test stimuli at a particular concentration was preceded by a standard isoamyl acetate stimulus, and a

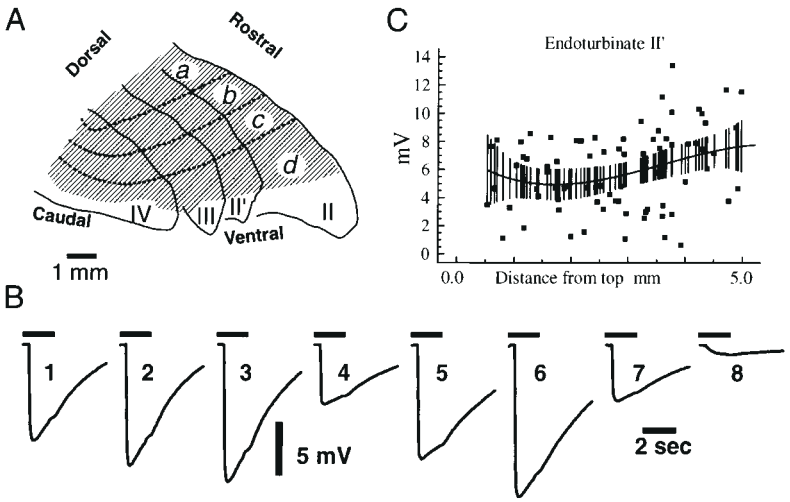

Figure 1 **(A)** Schematic representation of the medial surface of the turbinate bones. The Roman numerals indicate the turbinate bones (endoturbinate I was not recorded from because it was often damaged in the exposure of the other bones). The cross-hatching shows the extent of the epithelium from which we could reliably get responses. This corresponds to the region that stains with an antibody to olfactory marker protein (Vassar *et al.*, 1993). The lowercase letters (a–d) and dotted lines indicate the probable position of the gene expression zones judged from the literature (Vassar *et al.*, 1993). These will be referred to in this text as (a) extreme dorsal, (b) intermediate dorsal, (c) intermediate ventral and (d) extreme ventral to avoid confusion about the numbering systems used in different papers. **(B)** Individual, simultaneously recorded traces from a single eight-electrode array placed across the rostral border of endoturbinate IV. The number 1 electrode was the most dorsal and the number 8 electrode was the most ventral (except in Figure 2C). The analysis program reported the difference between the peak voltage and the mean voltage just before the response. The bars at the top of each trace show the 2 s period of isoamyl acetate odor presentation. The inflections on the falling phase of the responses correspond to the end of the odor pulse. This figure illustrates the variability in response to a single odor and the necessity for standardization of responses. The very small response from electrode 8 was taken just at the border of the color change at the ventral limit of the olfactory epithelium. **(C)** Distribution of unstandardized initial responses to isoamyl acetate across the rostral border endoturbinate II′. This includes all initial responses, including those with responses <4 mV, which were excluded from the data analysis. The vertical bars indicate the 95% confidence intervals for the curve. There is not significant slope to the curve.

blank was presented after each two-stimulus set. The odor was always presented for a 2 s period. Figure 1B shows that there was usually a peak response followed by a slow decline and a distinct inflection following odor removal. All odors were tested in groups of four odors: the standard odor (isoamyl acetate at a dilution of 10^{-1}) and three test odors over a series of descending dilutions from 1×10^{-1} to 1×10^{-4}. One and a half min elapsed after each stimulus presentation. A typical experiment began with two presentations of limonene, carvone and cineole odors at a dilution of 1×10^{-1}, followed by two descending sets of dilutions for these three odors. There was no effect of stimulus presentation order. In the text of this paper, we will refer to 1,8-cineole simply as cineole. The recording session usually lasted for 3–5 h. We sometimes ended an experiment earlier if the responses began to deteriorate badly on three or more electrodes. In some cases, the highest concentrations of the terpene compounds were tested before other odors were used that were outside the scope of this report. As a result, we have more extensive data for the higher concentrations than for the lowest concentrations.

The stimulus control differed from our previous papers in steps taken to improve the sharpness of the odor onset and to extend the intensity to lower dilutions. Odors were injected into a humidified, clean airstream flowing at 1000 ml/min. This airstream, in turn, flowed into a chamber with two large ports for clean air input and vacuum. Before each stimulus, the odor was turned on for 20 s to allow the build-up of the odor in the system. During this build-up period, the vacuum port was opened to draw the odor from the stimulus port and prevent stimulation. The vacuum line flowed in excess of 1000 ml/min. The actual rate was adjusted to give no EOG response at the onset of build-up or no upward drift at the presentation of blanks. Stimulation was applied to the epithelium by the closing of the vacuum port. This procedure is similar to that described previously (Kauer and Shepherd, 1975; Mackay-Sim and Kesteven, 1994). While some airflow transients occurred during these valve operations, the blanks usually produced responses of <0.4 mV. If the blanks became larger, the

Table 1 Concentrations for test odors at the peak dilution

Odor	Concentration (mol/l) at dilution of 10^{-1}	
	Observed	Calculated
Isoamyl acetate	5.6×10^{-5}	1.9×10^{-5}
Carvone	6.3×10^{-7}	4.2×10^{-7}
1,8-Cineole	6.3×10^{-6}	7.4×10^{-6}
Limonene	4.5×10^{-6}	7.8×10^{-6}

system was flushed with clean air to reduce contamination. Data were not used in the analysis if the standardized blank response was >1 mV or if the average response to the standard was <4 mV. (Large blank responses were observed only when the standard response was very large.)

Data analysis

The outputs were fed by an A/D converter (digitized at a rate of 26 Hz) to a computer that plotted the traces and computed the peak negative voltage relative to the baseline just before the stimulus. This peak voltage for each record was printed and stored in a file for later analysis. We inspected the plots for quality control during data collection and before analysis. Responses to all stimuli were standardized to the isoamyl acetate stimulus. The response to each odor was divided by the previous response to the standard stimulus at that electrode and was multiplied by the overall average response to the first isoamyl acetate (1×10^{-1}) responses from the first 10 experiments. This standard was chosen because it is a very commonly used stimulus and because it is very effective at all sites on the epithelium, even at relatively low concentrations. The isoamyl acetate response tended to be slightly larger in the ventral epithelium, but that increase was small relative to the variation. Therefore we have assumed an equal isoamyl acetate response at all sites, even though it may introduce a slight bias. Standardization helped minimize differences between recordings that might result from slight damage or drying at one site. It allowed us to adjust for the gradual run down of the response over the period of recording. As the tissue dried, one or more electrodes might lose contact with the tissue and the electrode would have to be advanced slightly to re-establish the recording. Response standardization allowed us to adjust for the resulting changes in response size.

It was not possible to visualize the receptor gene expression zones in adult animals. Therefore, we attempted to space the electrodes at equal distances across the turbinate bones in a direction that should cross the expression zones at nearly right angles. However, the difficulties of manipulating eight electrodes into a small space produced substantial variation in placement for different recording sessions on the same bone. Individual recording sessions could be analyzed by ANOVA to calculate the mean and confidence intervals. Response plots in single animals show the mean peak voltage at each electrode and concentration, and the 95% confidence intervals based on the standard error at that concentration and point. The mean blank response is illustrated for the highest flow rate through the clean odor bottle and is shown next to one of the sets of odor data. The blanks are not shown for composite curves for simplicity and because responses were selected to exclude any data with a large blank response.

Regression variables and contours

For statistical comparison of response variation across position and across recording sessions, we used stepwise polynomial regression instead of ANOVA. A photograph of each epithelium was made with the electrodes in place and the positions of the electrode tips were marked on this photograph. Photocopy enlargements were made of the marked photographs and a standard transparent overlay with x–y coordinates was used to record the positions of the tips. For analysis along the length of a single turbinate bone edge, the Euclidian distance from the most dorsal point of the slit between turbinate bones was used [$D = \sqrt{(x^2 + y^2)}$]. The first-, second- and third-order values of this distance were used in fitting lines through these points.

The mean peak voltage at each point was calculated and that value used as the response variable. Graphs of these inter-animal comparisons show individual points and the fitted line. The number of points is determined by the number of animals and the number of electrodes with good responses (isoamyl acetate response >4 mV and standardized blank response <1 mV).

Results

Effect of position in eight-electrode recording experiments

We restricted recordings to three terpene odors—limonene, carvone and cineole—because they gave distinctively different response profiles in earlier experiments (Scott *et al.*, 1997). Figure 2A,B shows recordings along the rostral edge of endoturbinate IV for one animal and endoturbinate II′ for a second animal. The figure shows the small amount of intra-animal variability that occurred in the standardized peak response as well as the typical low response to blanks. Responses to all odors increased with concentration. There was a larger response from the most dorsal region for carvone at all dilutions and this response fell steadily from the most dorsal to most ventral position. The limonene response was often smaller. When there was a spatial gradient for limonene, it was in the other direction (i.e. larger ventrally). The cineole response peaked at ~60–80% of the distance from the most dorsal site on the turbinate. This peak was large relative to the confidence intervals at all dilutions. The changes between regions of the epithelium were gradual. Although the response sizes varied as much as twofold, the changes were not abrupt.

We explored the caudal part of endoturbinate IV in several rats because the description of gene expression zones in the rat predicts a rostral-to-caudal as well as a dorsal-to-ventral pattern in that region (Vassar *et al.*, 1993) (also see Figure 1A). Figure 2C shows results from one session. Carvone at the highest concentration evoked the largest responses on the rostro-dorsal region of endoturbinate IV, and there was a peak in the profile at this position for all concentrations of carvone. The same region had the smallest responses for all concentrations of cineole and most concentrations of limonene. We were never able to place electrodes to span the entire caudal responsive region of endoturbinate

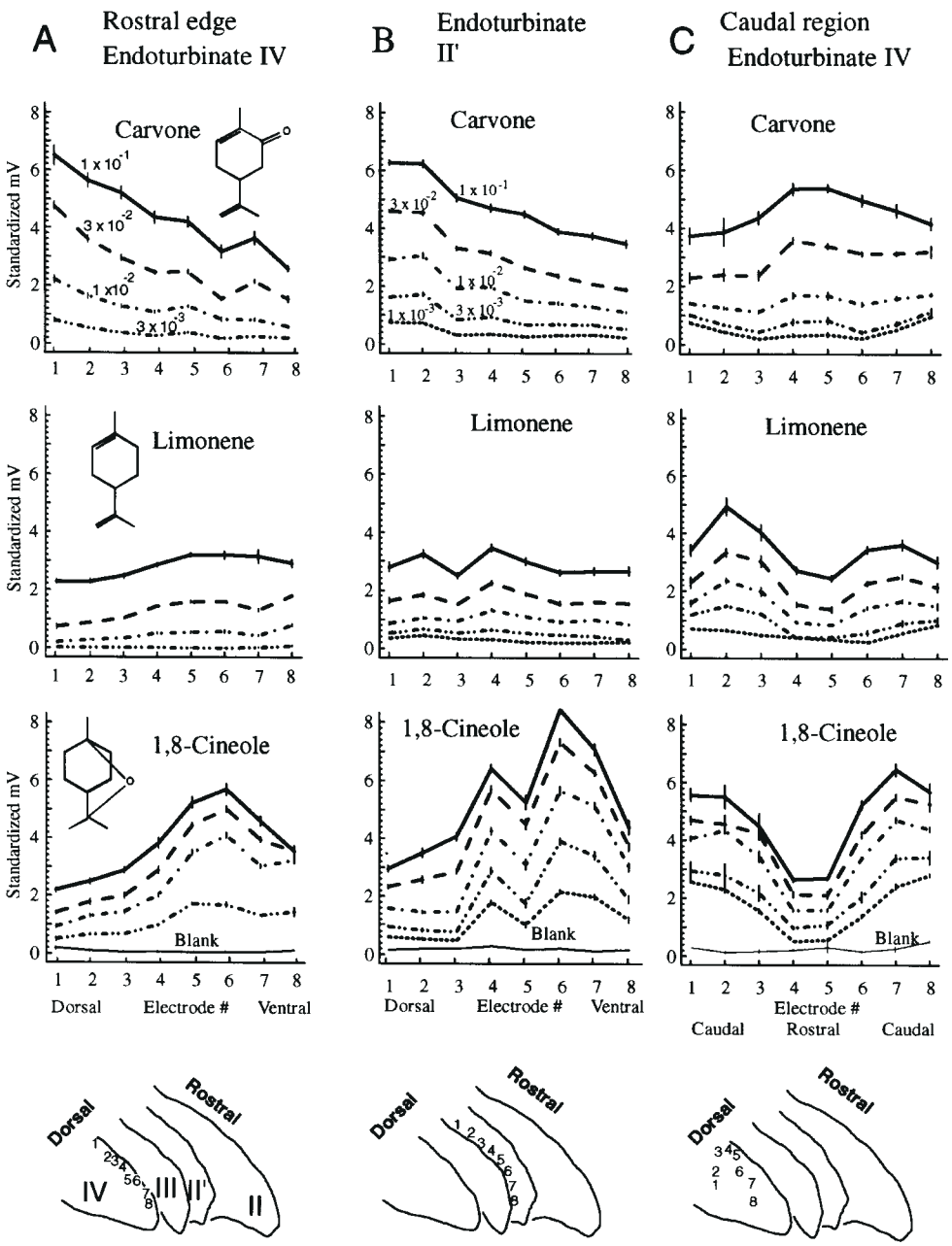

Figure 2 **Column A**. Response profiles from one recording session with four levels of odor concentration from endoturbinate IV (eight presentations of each odor dilution). The inset at the bottom of each column shows the electrode positions. Error bars are 95% confidence intervals. The concentration key for carvone applies to the other odors also. The blanks, illustrated with the cineole records, were generated by flowing air through a clean odor bottle at the highest rate used for odors. The chemical structure of the odors is shown next to the odor name in panel A. **Column B**. Response profiles from a single recording session with five levels of odor concentration from the dorsal edge of endoturbinate II′ (2–4 presentations of each odor dilution). The dip on electrode 5 in this animal was not a common feature, although there were some idiosyncratic dips or peaks in some the curves for individual preparations. **Column C**. Response profiles from one session in which the electrodes were arrayed across the rostral-to-caudal extent of endoturbinate IV (three presentations of each odor dilution). The stimulus concentrations are indicated by the same symbols as the other panels.

IV, but it was apparent that the cineole (and usually the limonene) response was smallest at the point of the peak carvone response.

These standardized results were generally stable despite the gradual rundown of the response over time. Figure 3 illustrates the first and last pairs of recordings from the rostral border of endoturbinate IV of a single animal, which were taken 3 h apart. These records are for the same three terpene odors at the highest concentration tested (10^{-1}). This figure shows another example of the gradients illustrated in Figure 2 and shows that the changes in profiles were small over that time period. This stability was present even when

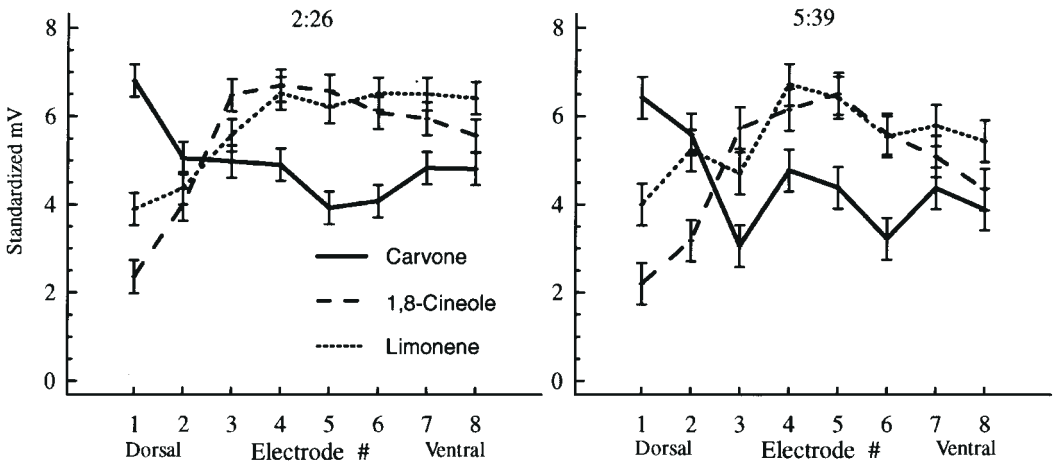

Figure 3 Illustration of stability of standardized response over time. The two sets of profiles are from a single preparation recorded along the rostral edge of endoturbinate IV >3 h apart. There were two stimulus presentations for each point on the plot.

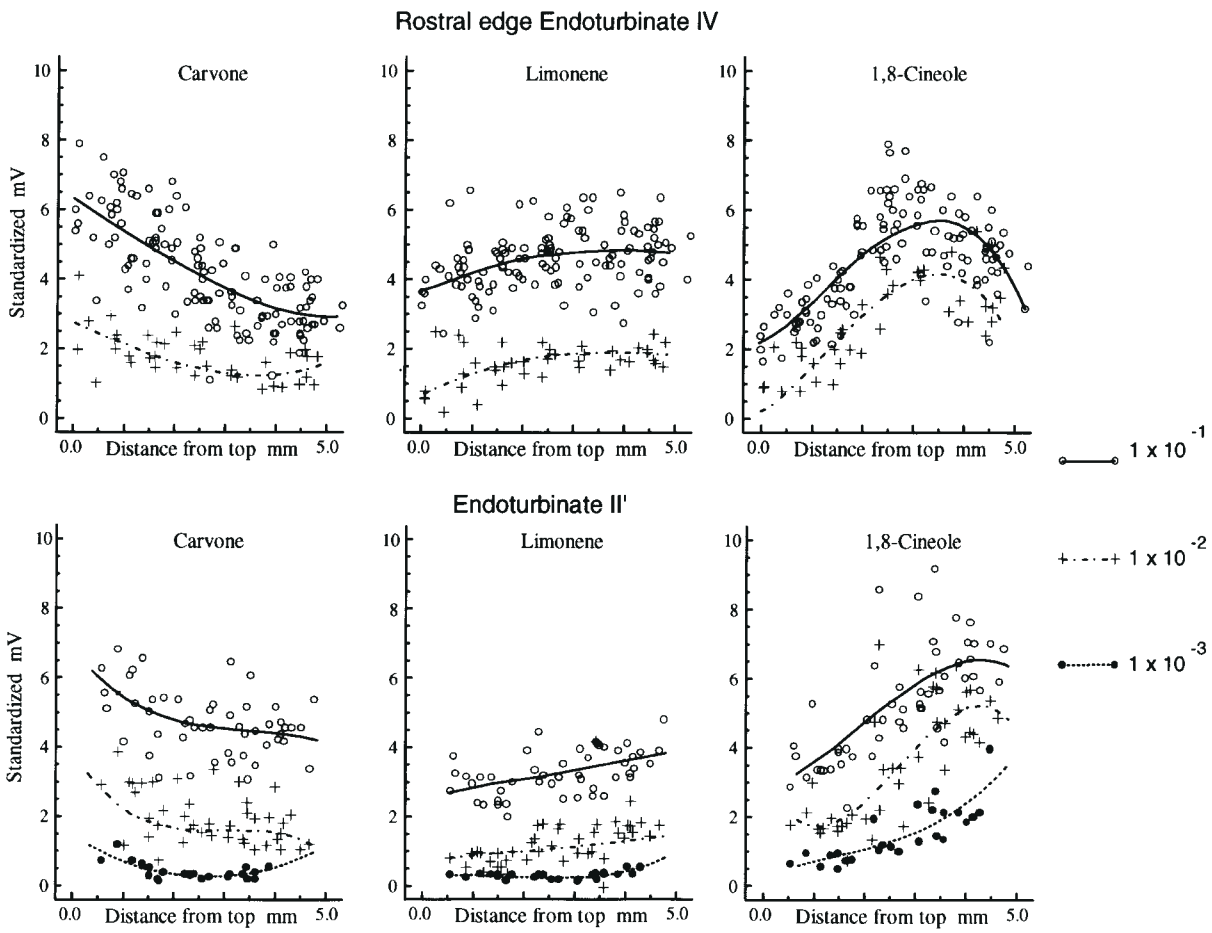

Figure 4 **Top**. Regression plots based on 16 animals for the rostral edge of endoturbinate IV. The lines were generally parallel. The stepwise polynomial regression procedure enters only those variables that make a significant contribution to the regression. **Bottom**. Regression plots for 11 sets of positions in eight animals from endoturbinate II′. The comparisons of slopes of the curves across the three odors are significantly different at each concentration. Although many animals were tested with all the concentrations indicated in Figure 2, only the results for 10^{-1}, 10^{-2} and 10^{-3} are shown to preserve clarity in the plots. Although a number of data points were collected at 10^{-3} on endoturbinate II′, not enough were collected on endoturbinate IV in this series to justify group curves at that concentration.

the absolute response declined by several millivolts. The standardized responses do not decline because they are based on comparison with the isoamyl acetate response.

Combined data across animals

In order to test whether there was consistency across animals, we used photographic measurements of electrode positions to overlay response plots. Figure 4 shows combined data from sets of sites recorded along the rostro-dorsal edges of endoturbinates IV and II′. In this figure, we have only used one dimension of the position, the distance from the most dorsal recording site on the particular endoturbinate. This figure shows that the curves representing the response profiles for the three odors are different. This is true for each of the two endoturbinate bones and for each concentration. The intermediate dilutions shown in Figure 2 were not included for clarity of the figure, but the curves were generally parallel to those shown. For the two dilutions shown for endoturbinate IV, there is a prominent inflection in the cineole curves showing a peak response somewhere above the most ventral recording sites. This peak is not clearly present in the group curves for endoturbinate II′, although it is present in most of the individual curves for both turbinate bones, as in Figure 2. Most of the individual profiles for cineole were similar to those for Figure 2A,B in that electrode 8 or electrodes 7 and 8 showed smaller responses than the immediately dorsal electrode. This was true for 90% of the rats in which we recorded from the rostral edge of endoturbinate IV. It was true for 73% recorded along endoturbinate II′ and 65% recorded along endoturbinate II.

The statistical significance of differences between curves was tested by making pairwise comparisons between the curves at each concentration on each of the two endoturbinate bones. Odor was used as a dummy variable (Kleinbaum and Kupper, 1978). A significant interaction at $P < 0.01$ was found between the dummy variable and the position variable in every case except for the comparison of carvone and limonene at 10^{-3} on endoturbinate II′.

Response maps

We summarized the recordings over a larger region of the epithelium by constructing maps from the x–y coordinates of the recording sites. Figure 5A illustrates those maps for two dilutions of the three terpene odorants. These maps show larger carvone responses on the dorsal regions of all turbinate bones. On endoturbinate IV, most of the larger carvone responses were found on the rostro-dorsal tip, corresponding to the pattern of the dorsal expression zone in neonatal rats (Vassar *et al.*, 1993). The limonene responses tend to be larger on the ventral parts of the turbinate bones and on the posterior part of endoturbinate IV, both regions where the carvone responses are smaller. The response gradients for cineole are steeper than those for limonene and, at least at the higher dilutions, show a decrease at the extreme ventral and posterior regions. We limited the figure to two dilutions for simplicity, but the responses at other odorant dilutions showed the same tendencies.

As noted for Figure 2, the pattern of responses on endoturbinate IV is more complicated than on endoturbinate II′, which is the other surface that was extensively sampled. The carvone responses became smaller for most points that were posterior and ventral to the rostro-dorsal edge. Limonene response generally became larger for the posterior ventral points. Cineole responses, particularly at the two highest concentrations, were larger on the center of the bone than on either the dorsal or ventral portions. This pattern follows that predicted from the receptor expression zone maps of Vassar *et al.* (Vassar *et al.*, 1993) summarized in Figure 1.

There is a suggestion in Figure 5 that the regions of maximal response to the three odors are not proportionally equal on the different turbinate surfaces. There were larger responses to cineole on endoturbinate II′ than on IV. The region of maximal cineole response also seems to extend more ventrally on II′, which is consistent with the difference between the cineole curves in Figure 6 and with the numbers of cineole profiles that show a prominent peak on the three turbinate surfaces. These differences must be interpreted cautiously. They could result from differences in the extent of the response zones to these odors, or they might result from differences in the response to the isoamyl acetate standardizing stimulus. A further caution is that points on different endoturbinate bones were recorded from different animals. However, reanalysis of the data of Scott *et al.* (Scott *et al.*, 1997) indicates a relatively larger cineole response compared with the limonene response on the more rostral endoturbinate bones (data not shown).

Recordings on other surfaces of the olfactory epithelium

Figure 6 shows one of two successful eight-electrode recordings from the nasal septum with the three terpene odors (the experimental set-up is shown in Figure 5B). We did not attempt to plot combined data for the two recordings because it was difficult to find reliable landmarks for lining up the recording sites. For the same reason, it is not possible to align these sites with the recordings from the endoturbinate bones. Nevertheless, the response patterns for the higher concentrations are similar to that seen in the previous figures, with carvone responses largest on dorsal sites, limonene responses largest in ventral sites and cineole responses peaking at intermediate sites.

We also made recordings from the dorsal, lateral surface of endoturbinate II in five animals. These were made in a different set-up because of the convenience of manipulating the electrodes into the requisite positions, and the olfactometer for that set-up did not extend to the lower concentrations. The preparation is illustrated in Figure 5C. We were able to produce overlays of photographs relying on

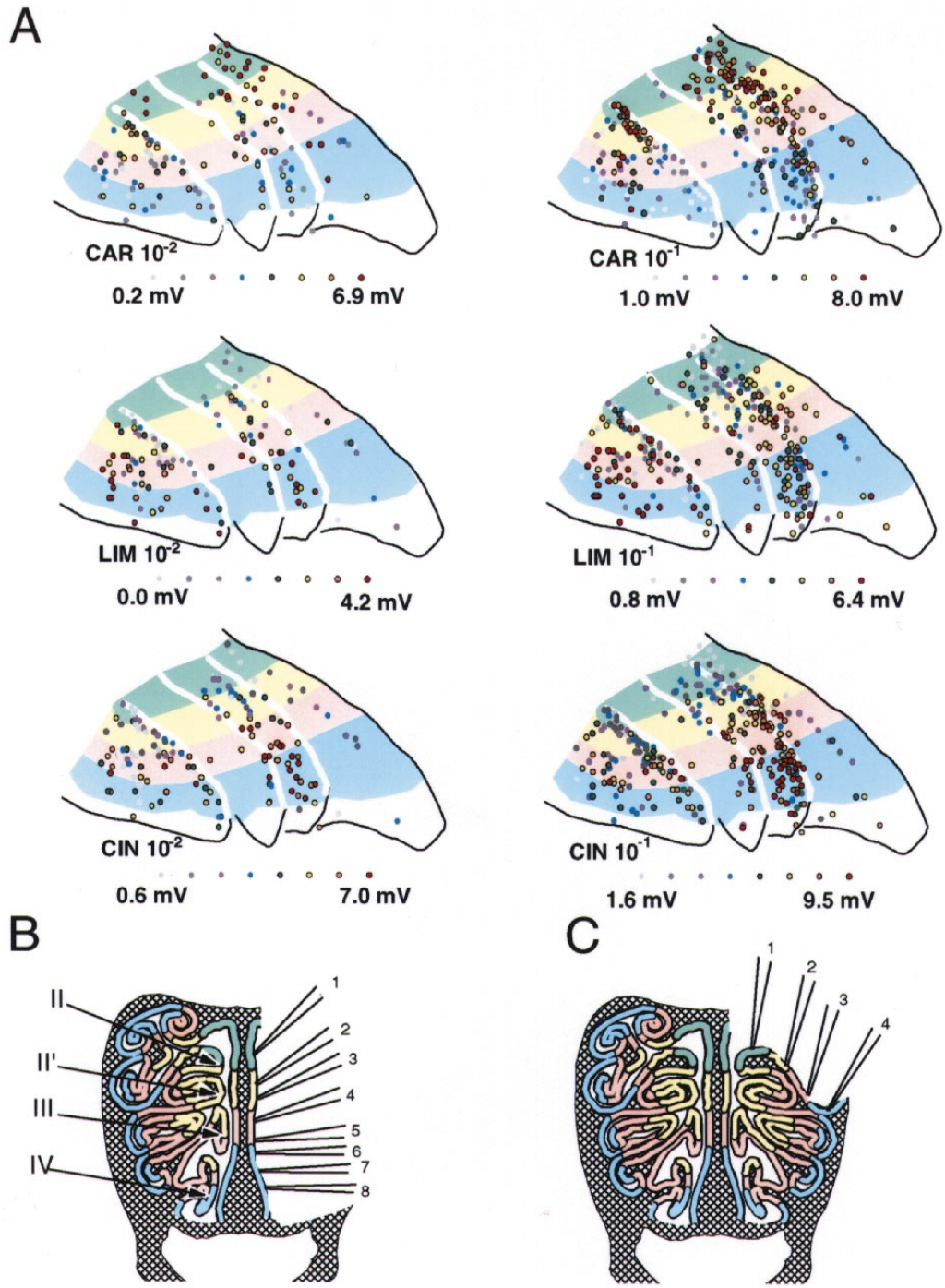

Figure 5 **(A)** Plots of response distributions to the three terpene odors across the medial surfaces of the endoturbinate bones. The bones are labeled in Figure 2. The range of responses for each odor and concentration are indicated in gray levels and colors below each plot. Each of the eight color gradations for each panel represents the size of standardized responses in intervals of 12.5%. The maximum and minimal standardized responses for each panel are indicated at the ends of the color scales. Points indicating responses above the mean for each plot have black surrounds. The column on the left illustrates responses to stimuli one log unit lower in concentration than those on the right. An intermediate concentration evoked similar distributions. This figure is based on placements in 60 animals. The background colors schematically indicate the expected position of the four expression zones described in the literature. These positions are estimated from published pictures of neonatal rats and mice (Ressler *et al.*, 1993; Vassar *et al.*, 1993). The fact that some substantial recordings were obtained below the site of the average estimated epithelium shows that these estimates were not perfectly accurate. **(B)** Approximate electrode placements for recordings along the nasal septum illustrated in Figure 6. **(C)** Approximate electrode placement for recordings along the dorsal surface of endoturbinate II′ illustrated in Figure 7. In B and C, the approximate positions of the neonatal expression zones are illustrated in colors matching those of the background colors in panel A.

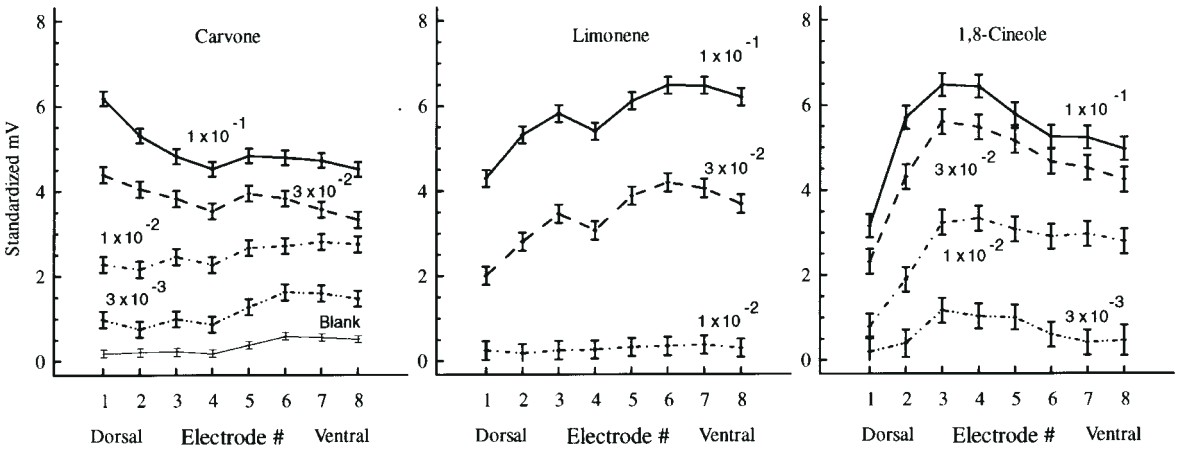

Figure 6 Concentration-by-electrode interaction plots for one animal with recordings from the nasal septum with electrodes arrayed in a dorsal-to-ventral direction. The error bars are 95% confidence intervals generated from an analysis of variance. The blank illustrated on the carvone curve represents air blown at the fastest rate (corresponding to the 1×10^{-1} level) through a clean bottle. Each odor was tested 12 times at each concentration. See Figure 5B for approximate electrode positions.

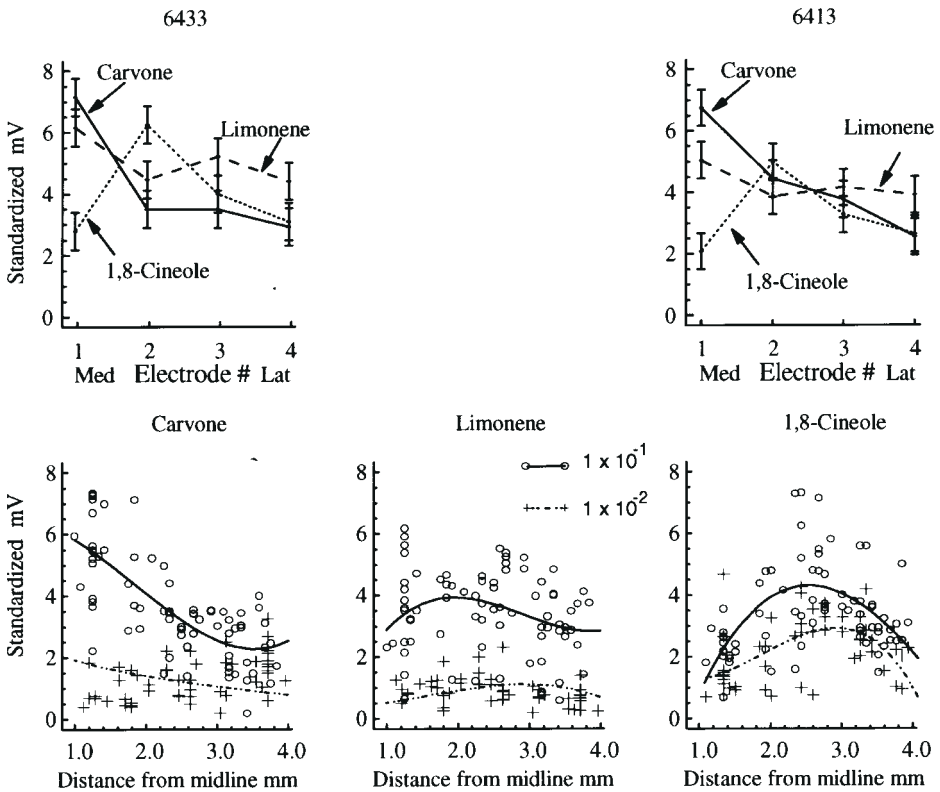

Figure 7 Distribution of responses from the dorsal, lateral surface of endoturbinate II. Data from seven animals with four electrodes in each case. Only three odor concentrations were used for most of these animals. See Figure 5C for approximate electrode positions.

the positions of exposed bones. Figure 7 displays individual data and the regression plots for these data. The response distributions were similar to those in the previous figures in that carvone produced larger responses at the medial sites and cineole produced the largest responses at intermediate sites. The limonene response distribution was flat and, for this odor only, none of the position parameters were significant for this odor. The comparisons of each pair of odor curves produced significant odor-by-position interactions ($P < 0.01$) by multiple regression except at the lowest

concentration, where the interaction for carvone versus limonene was significant at $P < 0.5$.

The lateral recordings confirm the differences between limonene and carvone response that were previously reported from intact animals (Scott *et al.*, 1996) and show that the limonene–carvone differences can exist even when the odor is directly applied to the exposed epithelium. This experiment also demonstrated a region of peak cineole sensitivity in the lateral region that was not obvious in the earlier recordings from intact animals.

Discussion

In this discussion, we will separate the empirical data about response distribution from the hypothesis of relation to receptor gene distribution by referring to 'regions' in describing the response data and 'zones' in discussing the published observations on gene expression patterns. Because we were unable to visualize the expression zones directly, it is important that we could test with a reasonable spatial resolution to evaluate whether there is a set of response regions that could correspond to the expression zones. We have previously argued that the response distributions may have their basis in chemical properties such as polarity or the presence of the carbonyl group (Scott *et al.*, 1996). By this logic carvone (a ketone) and limonene (a hydrocarbon) should have different response patterns. Cineole is a bicyclic ether and seems to have a more complex response distribution (Scott *et al.*, 1997).

Response distribution and gene expression zones

These data confirm and extend our previous conclusion that the adult rat olfactory epithelial responses to some odors are distributed in correlation with the neonatal olfactory receptor gene expression zones (Scott *et al.*, 1997). We had investigated the response profiles by placing one electrode on each of four endoturbinate bones and moving them sequentially from the ventral to dorsal position in seven steps. Thus all four electrodes were expected to correspond to a single expression zone. The responses to limonene were greatest in the ventral placements for all electrodes, and the responses to carvone were greatest in the dorsal placements for all electrodes. The effect of the dorsal-to-ventral position was confounded with the sequential electrode movement, and only a single concentration was used for each odor.

In the present study we doubled the number of simultaneous recordings. Within a single experiment, we arrayed the electrodes across the expected distribution of the gene expression zones. In single experiments, as well as in grouped analyses, we saw the regions of largest carvone response on the dorsal parts of the medial walls of the endoturbinate bones. The limonene response gradients were less pronounced, but there was a slight tendency for them to be largest ventrally. The cineole response was more complex, becoming largest in the ventral or intermediate ventral region. These results were in general correspondence with the gene expression zones described by Vassar *et al.* (Vassar et al., 1993). This correspondence existed even as the stimulus concentration was reduced. The correspondence also extended to other epithelial surfaces on the septum and the dorsal surface of endoturbinate II, extending out into the lateral recess.

These data do not test the number of response regions or whether the regions are discrete. The comparison of the carvone and cineole profiles suggests that there must be at least three different response regions. The observed profiles do not change in discrete steps. However, the gene expression zones do not have sharp boundaries (Vassar *et al.*, 1993). In addition, the length constant of the EOG recording from electrical stimulation of the epithelium is probably ~100 μm (Mackay-Sim and Kesteven, 1994). If the zones were equally represented across the 4 mm of recording distance, this space constant would represent ~10% of a zonal width. These two factors might account for the apparently gradual changes that we observed.

Other epithelial features are also distributed parallel to the receptor expression zones. Supporting cell morphology (Menco and Jackson, 1997), enzymatic activity in sustentacular cells (Miyawaki *et al.*, 1996), NADPH-diaphorase activity (Dellacorte *et al.*, 1995) and receptor guanylyl cyclase (Fülle *et al.*, 1995) have zonal distributions. Yoshihara *et al.* (Yoshihara *et al.*, 1997) found a zonal distribution for the adhesion molecule OCAM. Other factors, such as odorant binding proteins, could be distributed in a similar fashion (Rama Krishna *et al.*, 1995). Some of these factors might influence responses, even if the average specificity of odorant receptors did not change with expression zones. The fact that we have observed distinct spatial gradients for different types of odors makes this caution less convincing, but certainly does not remove it. On the other hand, the regional responses we find can be functionally important in determining the sensory input to the olfactory bulb irrespective of their origin.

Not all receptor genes are distributed according to the same zonal arrangement (Strotmann *et al.*, 1994; Kubick *et al.*, 1997; Ring *et al.*, 1997). Since only a few receptor genes have been studied by the *in situ* hybridization technique, it is possible that more deviations from the zonal arrangement will be found. This underscores the cautions about drawing the conclusion that our data necessarily reflect the properties of the receptor genes themselves, but does not detract from the fact that we have observed physiological properties that follow an important set of boundaries within the olfactory epithelium. It is possible that non-zonal receptor distributions may account for non-zonal response patterns observed for some odorants (Mackay-Sim and Kesteven, 1994; Youngentob *et al.*, 1995). There may be similar explanations for the small but consistent rostral-to-caudal relative difference in the cineole versus limonene responses.

The EOG technique cannot tell whether a larger response

for a particular odorant in one region comes from a small number of receptor cells that respond strongly to that odorant or from a large number of cells that respond weakly. These are questions that will have to be answered by techniques that measure individual cells or study receptors in expression systems (Raming *et al.*, 1993; Sato *et al.*, 1994; Rawson *et al.*, 1997; Wellerdieck *et al.*, 1997; Bozza and Kauer, 1998; Krautwurst *et al.*, 1998; Zhao *et al.*, 1998). So far, a complete answer to these questions has not emerged. Zhao *et al.* (Zhao *et al.*, 1998) measured EOGs and whole cell patch recordings of rat receptor cells transfected with a virus carrying the I7 receptor gene. They found increased responses to octanal and closely related aldehydes, but not to any others of a series of 74 odors, including fatty acids and alcohols. The I7 receptor is expressed in the most ventral zone (Vassar *et al.*, 1993). This is one contradiction to the expectation that more ventral receptors would respond to less polar odors (Scott *et al.*, 1996). Bozza and Kauer (Bozza and Kauer, 1998), on the other hand, found many examples of carvone responses in receptor cells projecting to the dorsal bulb, but no examples of limonene responses in the same cells. Krautwurst *et al.* (Krautwurst *et al.*, 1998) tested a set of 80 chimeric receptors containing the regions expected to code odorant recognition. They found a high degree of specificity among the 26 odorants that they tested with a cellular expression system. They confirmed the high selectivity reported for the I7 receptor in EOG experiments (Zhao *et al.*, 1998). These data suggest a narrow band of specificity for the olfactory receptors, at least in expression systems. This seems contrary to our previous speculation that many of the receptors in a particular expression zone might respond to a broad range of odorants with similar properties (Scott *et al.*, 1996).

Advantages and limitations of the EOG recording technique.

While the EOG recording procedure is limited in spatial resolution, it has distinct advantages. The recordings *in situ* avoid potential problems that may result from isolation of cells in artificial medium. Many odors can be tested over a series of concentrations. The preparation is simple and the responses in freshly killed animals are very similar to those in live animals (Scott *et al.*, 1996). Several different surfaces of the epithelium can be approached to test the correspondence with the gene expression zones, as we have done for the terpene odors in this paper. We propose that any claim of full correlation with the expression zones ought to test several such surfaces.

The EOG recording technique is very sensitive to tissue exposure, to mechanical damage, to the exact depth of the electrode and to drying. Some of these problems were accentuated in the placement of eight simultaneous electrodes. Standardization of the response is very useful for comparing responses across electrodes and across animals. The choice of the standardizing stimulus would alter the shape of the profiles, but would not alter the fact that the profiles are different for different odors. On average, the isoamyl acetate response has been a little larger ventrally than dorsally. Consequently, the absolute odor profiles collected under ideal conditions might differ from the standardized profiles shown here. We have implicitly assumed that there is no difference in the isoamyl acetate response from one turbinate bone to another. The large response variation in Figure 1C shows how difficult the absolute response is to assess. Other authors (Mackay-Sim and Kesteven, 1994; Youngentob *et al.*, 1995) presented data indicating that the average size of amyl acetate responses changes substantially across the rat epithelium, but those data disagree strongly about the regions of maximal response.

The use of multiple electrodes allows a comparison of odorant series or concentrations within a single animal. This is a faster procedure than exploring many sites with a single electrode (Mackay-Sim and Kesteven, 1994) and avoids introduction of variance from moving the electrode. The multi-animal regression plots show that the relationships seen in single animals are repeatable. The hypothesis of zonal expression is essential to making comparisons of responses to an odorant series in single animals, because it allows electrodes to be placed linearly without the necessity of sampling the entire epithelium. Therefore, hypotheses about the regional distribution of responses to a series of compounds can reasonably be tested in single preparations.

We propose that this preparation will be useful for screening the mass response to odors across the expression zones. Such data could show which odors are likely to be strong ligands for receptors expressed in particular zones. In addition, as noted above, studies on isolated receptor cells or on receptor genes expressed in non-olfactory cell lines will not be subject to the enzymes or other factors expressed locally in olfactory receptor cells or surrounding tissue. If these turn out to be significant in determining the response, then it will be necessary to study receptor cell processes *in situ* if we are to understand the pattern of sensory input to the olfactory bulb.

Acknowledgements

Supported by National Institute of Deafness and Other Communications Disorders Grant DC00113. The authors thank F.H. Schmidt for aid with instrumentation and consultation about data analysis and D. Blakley who performed the lateral recordings. We thank D. Wellis, P. Ezeh, M. Singer, N. Buonviso and M. Chaput for reading earlier drafts of the manuscript.

References

Astic, L., Saucier, D. and **Holley, A.** (1987) *Topographic relationships between olfactory receptor cells and glomerular foci in the rat olfactory bulb*. Brain Res., 424, 144–152.

Bozza, T.C. and **Kauer, J.S.** (1998) *Odorant response properties of convergent olfactory receptor neurons.* J. Neurosci., 18, 4560–4569.

Dellacorte, C., Kalinoski, D.L., Hugue, T., Wysocki, L. and **Restrepo, D.**

(1995) *NADPH diaphorase staining suggests localization of nitric oxide synthase within mature vertebrate olfactory neurons*. Neuroscience, 66, 215–225.

Ezeh, P.I., Scott, J.W. and **Davis, L.M.** (1995) *Regional distribution of rat electroolfactogram.* J. Neurophysiol., 73, 2207–2220.

Fülle, H., Vassar, R., Foster, D.C., Yang, R., Axel, R. and **Garbers, D.L.** (1995) *A receptor guanylyl cyclase expressed specifically in olfactory neurons.* Proc. Natl Acad. Sci. USA, 92, 3571–3575.

Guthrie, K.M., Anderson, A.J., Leon, M. and **Gall, C.** (1993) *Odor-induced increases in* c-fos *mRNA expression reveal an anatomical 'unit' for odor processing in olfactory bulb*. Proc. Natl Acad. Sci. USA, 90, 3329–3333.

Imamura, K., Mataga, N. and **Mori, K.** (1992) *Coding of odor molecules by mitral/tufted cells in rabbit olfactory bulb. I. Aliphatic compounds*. J. Neurophysiol., 68, 1986–2002.

Kauer, J.S. and **Shepherd, G.M.** (1975) *Olfactory stimulation with controlled and monitored step pulses of odor*. Brain Res., 85, 108–113.

Kleinbaum, D.G. and **Kupper, L.L.** (1978) Applied Regression Analysis and Other Multivariable Methods. Duxbury Press, North Scituate, MA.

Krautwurst, D., Yau, K.-W. and **Reed, R.R.** (1998) *Identification of ligands for olfactory receptors by functional expression of a receptor library*. Cell, 95, 917–926.

Kubick, S., Strotmann, J., Andreini, I. and **Breer, H.** (1997) *Subfamily of olfactory receptors characterzed by unique structural features and expression patterns*. J. Neurochem., 69, 465–475.

Lancet, D., Kauer, J.S. and **Greer, C.A.** (1981) *High resolution 2-deoxy-glucose localization in olfactory epithelium.* Chem. Senses, 6, 343–349.

Leveteau, J. and **MacLeod, P.L.** (1966) *Discrimination des odeurs par les glomérules olfactifs du lapin (étude électrophysilogique).* J. Physiol. (Paris), 58, 717–729.

Mackay-Sim, A. and **Kesteven, S.** (1994) *Topographic patterns of responsiveness to odorants in the rat olfactory epithelium*. J. Neurophysiol., 71, 150–160.

Menco, B.P. and **Jackson, J.E.** (1997) *A banded topography in the developing rat's olfactory epithelial surface*. J. Comp. Neurol., 388, 293–306.

Miyawaki, A., Homma, H., Tamura, H. and **Mikoshiba, K.** (1996) *Zonal distribution of sulfotransferase for phenol in olfactory sustentacular cells.* EMBO J., 15, 2050–2055.

Mombaerts, P., Wang, F., Dulac, C., Chao, S.K., Nemes, A., Mendelsohn, M., Edmondson, J. and **Axel, R.** (1996) *Visualizing an olfactory sensory map*. Cell, 87, 675–686.

Mori, K. and **Yoshihara, Y.** (1995) *Molecular recognition and olfactory processing in the mammalian olfactory system*. Prog. Neurobiol., 45, 585–619.

Nef, P., Hermans-Borgmeyer, I., Artieres-Pin H., Beasley, L., Dionne, V.E. and **Heinemann, S.F.** (1992) *Spatial pattern of receptor expression in the olfactory epithelium.* Proc. Natl Acad. Sci. USA, 89, 8948–8952.

Pedersen, P.E., Jastreboff, P., Stewart, W.B. and **Shepherd, G.M.** (1986) *Mapping an olfactory receptor population to a specific region in the rat olfactory bulb.* J. Comp. Neurol., 250, 93–108.

Rama Krishna, N.S., Getchell, M.L., Margolis, F.L. and **Getchell, T.V.** (1995) *Differential expression of vomeromodulin and odorant-binding protein, putative pheromone and odorant transporters, in the developing rat nasal chemosensory mucosae*. J. Neurosci. Res., 40, 54–71.

Raming, K., Krieger, J., Strotmann, J., Boekhoff, I., Kubick, S., Baumstark, C. and **Breer, H.** (1993) *Cloning and expression of odorant receptors.* Nature, 361, 353–356.

Rawson, N.E., Gomez, G., Cowart, B., Brand, J.G., Lowry, L.D., Pribitkin, E.A. and **Restrepo, D.** (1997) *Selectivity and response characteristics of human olfactory neurons.* J. Neurophysiol., 77, 1606–1613.

Ressler, K.J., Sullivan, S.L. and **Buck, L.B.** (1993) *A zonal organization of odorant receptor gene expression in the olfactory epithelium*. Cell, 73, 597–609.

Ressler, K.J., Sullivan, S.L. and **Buck, L.B.** (1994) *Information coding in the olfactory system: evidence for a stereotyped and highly organized epitope map in the olfactory bulb*. Cell, 79, 1245–1255.

Ring, G., Mezza, R.C. and **Schwob, J.E.** (1997) *Immunohistochemical identification of discrete subsets of rat olfactory neurons and the glomeruli that they innervate*. J. Comp. Neurol., 388, 415–434.

Sato, T., Hirono, J., Tonoike, M. and **Takebayshi, M.** (1994) *Tuning specificities to aliphatic odorants in mouse olfactory receptor neurons and their local distribution*. J. Neurophysiol., 72, 2980–2989.

Schoenfeld, T.A., Clancy, A.N., Forbes, W.B. and **Macrides, F.** (1994) *The spatial organization of the peripheral olfactory system of the hamster. Part I. Receptor neuron projections to the main olfactory bulb*. Brain Res. Bull., 34, 183–210.

Scott, J.W., Davis, L.M., Shannon, D. and **Kaplan, C.** (1996) *Relation of chemical structure to spatial distribution of sensory responses in rat olfactory epithelium*. J. Neurophysiol., 75, 2036–2049.

Scott, J.W., Shannon, D.E., Charpentier, J., Davis, L.M. and **Kaplan, C.** (1997) *Spatially organized response zones in rat olfactory epithelium.* J. Neurophysiol., 77, 1950–1962.

Strotmann, J., Wanner, I., Helfrich, T., Beck, A., Meinken, C., Kubick, S. and **Breer, H.** (1994) *Olfactory neurones expressing distinct odorant receptor subtypes are spatially segregated in the nasal neuroepithelium.* Cell Tissue Res., 276, 429–438.

Vassar, R., Ngai, J. and **Axel, R.** (1993) *Spatial segregation of odorant receptor expression in the mammalian olfactory epithelium*. Cell, 74, 309–318.

Vassar, R., Chao, S.K., Sitcheran, R., Nuñez, J.M., Vosshall, L.B. and **Axel, R.** (1994) *Topographic organization of sensory projections to the olfactory bulb.* Cell, 79, 981–991.

Wang, F., Nemes, A., Mendelsohn, M. and **Axel, R.** (1998) *Odorant receptors govern the formation of a precise topographic map.* Cell, 93, 47–60.

Wellerdieck, C., Oles, M., Pott, L., Korsching, S., Gisselmann, G. and **Hatt, H.** (1997) *Functional expression of odorant receptors of the zebrafish* Danio rerio *and of the nematode* C. elegans *in HEK293 cells*. Chem. Senses, 22, 467–476.

Youngentob, S.L., Kent, P.F., Sheehe, P.R., Schwob, J.E. and **Tzoumaka, E.** (1995) *Mucosal inherent activity patterns in the rat, evidence from voltage-sensitive dyes.* J. Neurophysiol., 73, 387–398.

Yoshihara, Y., Kawasaki, M., Tamada, A., Fujita, H., Hayashi, H., Kagamiyama, H. and **Mori, K.** (1997) *OCAM: A new member of the neural cell adhesion molecule family related to zone-to-zone projection of olfactory and vomeronasal axons*. J. Neurosci., 17, 5830–5842.

Zhao, H., Ivic, L., Otaki, J.M., Hashimoto, M., Mikoshiba, K. and **Firestein, S.** (1998) *Functional expression of a mammalian odorant receptor.* Science, 270, 237–242.

Accepted June 24, 1999